PROCEEDINGS OF ECOS 2023 - THE 36TH INTERNATIONAL CONFERENCE ON
EFFICIENCY, **C**OST, **O**PTIMIZATION, **S**IMULATION AND ENVIRONMENTAL IMPACT OF ENERGY SYSTEMS
25-30 JUNE 2023, LAS PALMAS DE GRAN CANARIA, SPAIN

Optimal integration of Power-to-Gas and district heating through waste heat recovery from electrofuel production

Agostino Gambarotta[a], Francesco Ghionda[a], Emanuela Marzi[a], Mirko Morini[a] and Costanza Saletti[a]

[a] *University of Parma, Parma, Italy, agostino.gambarotta@unipr.it; francesco.ghionda@studenti.unipr.it; emanuela.marzi@unipr.it,**CA**; mirko.morini@unipr.it; costanza.saletti@unipr.it*

Abstract:

The growing penetration of renewable energies, which have a fluctuating nature, requires the enhancement of energy system flexibility. This can be achieved through sector integration, which encompasses the conversion of energy into the most convenient vectors. In this regard, a promising option is represented by Power-to-Gas (PtG) technologies. They allow the direct conversion of surplus renewable electricity into fuels (e.g. green hydrogen or methane) and its long-term storage, operating as seasonal storage. The potential of PtG systems can be unlocked if the waste heat produced by exothermic components (e.g. electrolyzer and methanation reactor) is recovered and fed, for instance, into a district heating network (DHN) to be supplied to an end-user. However, since the operation of PtG systems may be discontinuous, a full integration of the fuel, electrical and heating sectors is possible only with advanced management and control tools. This work presents a control strategy based on Model Predictive Control, with the aim of operating the production of methane from a PtG system and the supply of waste heat to a DHN with minimal cost. The case study comprises an electrolyzer, a methanation reactor, storage tanks for hydrogen and methane, a boiler and a heat pump for upgrading the temperature level of the recovered heat. The controller feasibility is demonstrated through a Model-in-the-Loop simulation platform and its performances are compared to that obtained with a conventional controller. The novel controller enables a 54 % increase in operating margin and more than halves carbon dioxide emissions. A better exploitation of renewable energy is also obtained (+ 4.6 %), as well as an increase in the share of heat recovered from the PtG plant.

Keywords:

District Heating Network; Electrolyzer; Methanation; Model Predictive Control; Power-to-Gas; System Integration; Waste Heat Recovery.

1. Introduction

Due to the need to decarbonize the energy sector, a great effort is being made today to support the penetration of renewable energy sources (RES), and this is transforming the architecture of current energy systems. Indeed, the mismatch between energy production and demand creates challenges that add complexity and forces the integration of new technologies and solutions. This leads to a change in the conventional way of managing energy systems, and to the need to exploit the concept of Multi-Energy Systems (MES), which means to consider energy systems as a whole, and therefore to perform an overall optimization of energy exchanges, including sector integration.

Power-to-Gas (PtG) technologies are gaining importance in this context, enabling sector coupling through the production of synthetic fuels (i.e. electrofuels) from renewable electricity, as demonstrated by many ongoing research activities on this topic [1]. Electrofuels can be used as conventional fuels and even converted back into electricity when necessary: thus, they can serve as an energy storage solution avoiding renewable energy curtailments. As expected, the total efficiency of the process is low, but it can be increased by making profitable use of the waste heat. Indeed, being an exothermic process, when integrated into an energy system, a PtG plant can also provide additional heat to be used by the end-users. Böhm et al. [2] studied the potentials of coupling Power-to-Hydrogen with a District Heating Network (DHN), finding that there are several synergies and efficient interactions between them. While high-temperature electrolysis is comparable with industrial waste heat, low-temperature electrolysis is subject to infrastructure limitations: however, the modern low-temperature DHN represent an opportunity for its usage.

Due the complexity presented above, it is evident that when dealing with the problem of the future management of PtG systems integrated into MES, the control of such systems plays a key role. Indeed, how a PtG unit is integrated into the system and how it is operated, strongly influence its potential. Fischer et al. [3] found that Model Predictive Control (MPC) is a suitable control strategy for optimizing the operation of PtG technologies, mainly when such systems are integrated into complex MES. They successfully demonstrated the application

https://doi.org/10.52202/069564-0221

of an MPC for optimizing the operation of a PtG unit and on-site storage considering the limitations in energy networks and time variable electricity prices. Turk et al. [4] studied the application of an MPC for a system with PtG and gas storage for system flexibility, considering multiple uncertainties. The authors found that the MPC made it possible to reduce the wind curtailment and improve the economic performance of the system, compared with a traditional control strategy. They also investigated the impact of the MPC prediction horizon length on computational efficiency, finding that it should be selected based on the required computational efficiency and storage capacity of the system. Finally, Abdelghany et al. [5] investigated the implementation of a two-stage MPC for the integration of a PtG plant for hydrogen production from a wind farm, to be used for hydrogen-fueled road vehicles or for injection into the local grid. By using a two-stage predictive controller, they tackled different competing objectives and different time-scales, and optimally managed the interactions between the wind farm, end-user and power grid. As demonstrated by these studies, an intelligent control strategy is needed to successfully manage such systems. However, in the presented papers, the possibility of recovering the waste heat of the PtG plant was not considered.

Waste heat recovery was nonetheless studied by Huang et al. [6]. The authors analyzed the benefits of using a Mixed-Integer Linear Programming (MILP)-based economic MPC for the real time control of complex MES integrated with the production of hydrogen. They recovered the waste heat of a high temperature alkaline electrolyzer and used it directly in a DHN, achieving cost savings and a better exploitation of RES, compared to a conventional rule-based strategy.

Given the necessity to decarbonize current energy systems, a great effort is being made today in studying and applying novel control strategies and optimization tools in real systems for the integration of new technologies and for the exploitation of sector coupling. Nevertheless, being a complex problem, with many degrees of freedom, it is necessary to keep studying different applications and the benefits of the integration of PtG technologies in energy systems. In particular, considerable effort is still needed in the study of the smart management of PtG plants and of waste heat recovery from it, in order to exploit all the potentials of this technology.

The main contributions of this paper are the following:

- The development of a novel MPC controller with an integrated MILP algorithm for the optimal control of a PtG plant for the production of methane, coupled with a DHN for waste heat recovery.
- An innovative solution for recovering the waste heat from the PtG plant. A heat recovery circuit (HRC), which works at low temperatures, i.e. (40÷55) ℃, is used to recover the waste heat of the PEM electrolyzer, the methanation reactor and the condenser, and then the low-temperature heat at 55 ℃ is upgraded by an industrial heat pump (HP) and is used in a DHN, as outlined in Figure 1.
- The quantification of the benefits of using the innovative control solution, compared to a conventional rule-based control strategy, by the implementation of both solutions in a Model-in-the-Loop (MiL) configuration.

2. Method

This section presents the methods exploited in this work: the concept of MPC, the optimization algorithm developed for its implementation and the detailed model used for the MiL application.

2.1. Model Predictive Control

The optimal control of a MES using smart control strategies is becoming more and more common and it is catching the attention of researchers and industries. Indeed, when using advanced control strategies, it is possible to perform the optimal management of complex systems, which follows the implemented objectives (such as cost or energy consumption minimization).

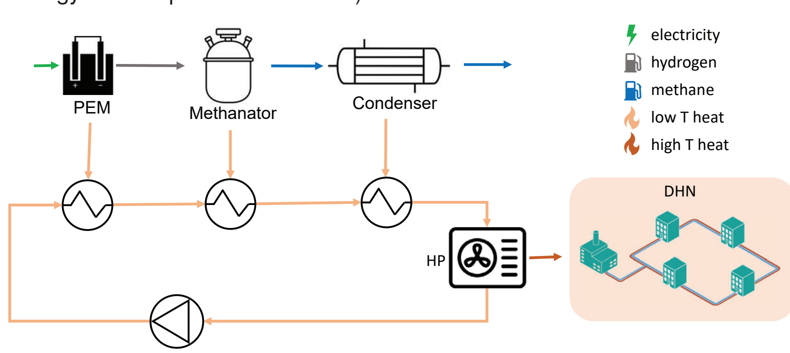

Figure 1: A schematic representation of the heat recovery from the Power-to-Gas plant.

 https://doi.org/10.52202/069564-0221

MPC is a smart control strategy that has been demonstrated to be successful for many applications [7]. In this type of controllers, an optimization algorithm is embedded, which includes a simplified model of the system to control. At every time-step, the algorithm receives information on the actual behavior of the system, and calculates an optimal trajectory for the inputs over a future time-horizon, also known as prediction horizon, which is discretized into a certain number of time-steps. From this trajectory, only the first signal is implemented into the real system (e.g. as a set-point in low-level controllers), and after a time-step is passed, the system states are estimated and given again to the controller, together with the forecast of the disturbances, which repeats the calculation for a new prediction horizon.

With this control strategy, an optimal control of the system is allowed: the controller gives the optimal inputs to the system every time-step (e.g. 15 minutes), and there is an implicit feedback and feed-forward on the disturbances. Nevertheless, an adequate algorithm is needed to use this control strategy, which has to be fast and contain the model of the system to control. In this work, a MILP algorithm is used, which is described in detail in Paragraph 2.2.. The aforementioned advantages of using this technique, such as the consideration of the predicted disturbances, the possibility to handle constraints and the concomitant optimization, make MPC a suitable control technique for MES [6].

2.2. Optimization algorithm

As explained above, to develop an MPC controller, an optimization algorithm is required. It is embedded in the controller and calculates the optimal future trajectory for the control variables. Moreover, the algorithm needs to be fast, since it is run at every time-step, and needs to optimize the system over the entire prediction horizon. Among the existing optimization algorithms, the Mixed-Integer Linear Programming technique has revealed to be a successful optimization model for MES, if properly tailored to the case study. Indeed, this strategy makes it possible to optimize the systems with good accuracy and reasonable computational complexity. In addition, efficient commercial solvers are available for such problems, and the global optimality of the solution is guaranteed [8]. When using such approach, the equations that describe the physical behavior of the system must be linear, and therefore they need to be linearized. It is possible to model a general MES using the following components:

- **Conversion systems**: they represent all the plants involved, which transform the energy from one (or more) form to another one (or more), e.g. boilers, heat pumps, electrolyzers. To model them, the input-output relationship is linearized, and piecewise linearization can be used to consider variations in efficiency with the load [9, 10]. This formulation needs auxiliary variables and constraints, which are described in detail in [11]. Moreover, when necessary, the piecewise linearization has been performed on two variables (e.g. to model the compressor, the electrical energy used depends both on the gas mass flow rate and on the pressure ratio). While the piecewise linearization of one-degree of freedom performance curves is relatively straightforward, when the piecewise linearization is made on two variables, several piecewise linear approximation approaches exist. In this work, the triangle method was applied to those components that needed it [11]. In addition, for each plant, three operating modes can be modeled (ON, OFF and standby), and it is possible to set a start-up cost, as well as a minimum up-time (UT) and down-time (DT), and operating ramps, by adding additional equations and binary variables to the problem.
- **Energy storages**: they represent every component that can store energy, e.g. batteries, thermal energy storages, gas storage tanks. The equation that describes them relates the energy stored at the current time-step to the one stored at the previous time-step, by taking into account charge, discharge and self-discharge efficiencies.
- **Energy networks**: they are modeled as energy sinks/sources, to/from which the energy system can exchange energy by buying or selling it with certain costs, e.g. electricity grids, natural gas networks.
- **End-users and RES**: they are modeled as energy sinks/sources, with the needs to be fulfilled or the production rate given as disturbances to the algorithm.
- **Energy nodes**: they are not physical nodes, however, they are used to make sure the energy balance for each energy vector is fulfilled every time-step.

The optimization variables are all the power flows and the energy stored, and the algorithm calculates their optimal management for each time-step, in order to minimize the implemented objective function over the prediction horizon.

2.3. Simulation platform

As previously mentioned, the management presented was tested in a Model-in-the-Loop configuration. A detailed nonlinear model, which emulates the real system, was developed in the MATLAB®/Simulink® environment, and it was built by assembling the models of single energy system components. The application

https://doi.org/10.52202/069564-0221

consists of a wind farm, a PtG system for the production of synthetic methane and a DHN, which ensures heat supply to an end-user.

The Simulink® library used to model the DHN has already been presented in previous works [12], and it is composed of the pumping station blocks (expansion vessels and pumps), the heating network blocks (pipelines) and the thermal power unit blocks (boilers and heat exchangers). Nevertheless, for the present application, new components were developed, that constitute the PtG plant. The main components and how they were modeled is presented below.

Wind farm: this is an algebraic model which, starting from the undisturbed wind velocity module and direction $\mathbf{u}_{wind}$, and given the geometry of the wind turbines and their position in the wind farm, calculates the output electrical power production. It considers the wake effect by applying the Jensen wake model [13] and once the corrected wind velocity $\mathbf{u}_{wind_{corr}}$ for each turbine is determined, uses the power curve of the turbines to calculate the electricity generated: $P_{el} = f(\mathbf{u}_{wind_{corr}})$.

PEM electrolyzer: this is an algebraic model that, given the electrical power supplied and the operating mode returns the amount of hydrogen and the thermal power generated. It has three different operating modes: ON, OFF (i.e. no consumption, no production, cold start-up needed to switch on) and standby (i.e. no production, consumption of a certain amount of nominal electrical power, warm start-up needed to switch on). During the steady state operation, the relation for the efficiency of the electrolyzer is derived by interpolating operating data

$$\eta = \rho HHV \frac{aP_{el}^{b} + c}{P_{el}}, \tag{1}$$

and it is used to calculate the hydrogen flow rate produced as follows

$$\dot{V}_{H_2} = \frac{1}{\rho HHV}\eta P_{el}, \tag{2}$$

with ρ being the gas density, HHV its high heating value and P_{el} the input electrical power. The thermal power generated is calculated using the following equation

$$P_{th} = (1 - \eta)P_{el} - P_{loss}, \tag{3}$$

where P_{loss} represents the power loss and is calculated as $P_{loss} = \alpha P_{nom} + \beta P_{el} + \gamma P_{nom}$: the first term represents the losses due to the auxiliary systems, while the latter terms represent the linear model of the power losses in the conversion from AC to DC.

Methanation reactor: this is an algebraic model that correlates the input hydrogen flow to the output methane flow and thermal power generated. Similarly to the electrolyzer, it has three operating modes: ON, OFF and standby. In the steady state operation, the output flow is calculated using the yield of reaction y, which is estimated based on linear interpolation of experimental data as follows

$$y = a\frac{GHSV}{GHSV_{nom}} + b \tag{4}$$

where GHSV (gas hourly space velocity) is the rate between the total volumetric flow rate at inlet and the reactor's volume, and evaluates the load of the reactor.

Gas compressor: this is an algebraic model that, given the rotational speed, the input flow and the output desired pressure, calculates the output flow and the electrical power consumption. The block contains the performance maps of the turbocompressor for the calculation of the mass flow rate and of the polytropic efficiency, given the corrected rotational speed and the pressure ratio.

Gas storage: the proposed model represents a node in which the input flow is mixed with the gas inside the storage. It is a dynamic model that uses the energy balance and continuity equations for pressure and temperature calculation. In terms of causality, the incoming and outcoming flows are known, and the model calculates the pressure, temperature and composition of the gas contained in the storage. The energy stored is calculated using the gas HHV.

Gas pipeline: this is a dynamic model which, given the inlet pressure, temperature and composition, and the outlet pressure, calculates the output mass flow rate, temperature and composition of the gas. The mass flow rate is calculated as follows

$$\dot{m} = sign(\Delta p)\sqrt{\frac{|\Delta p|\rho A_{cs}}{\frac{\lambda L}{D_{in}} + Z}}, \tag{5}$$

 https://doi.org/10.52202/069564-0221

where Δp is the pressure drop in the pipeline, A_{cs} the cross-section area of the pipeline, ρ the gas density, λ the friction factor, L the pipe length, D_{in} the inner diameter, and Z the total concentrated pressure drop. The governing equation for the temperature is the following

$$\frac{dT_{out}}{dt} = \frac{1}{\rho c_v V}\left(\dot{m}\left[(c_p T)_{in} - (c_p T)_{out}\right] - \dot{Q}_w\right), \tag{6}$$

where c_p is the gas specific heat at constant pressure, c_v the average gas specific heat at constant volume, V the volume of the pipeline and $\dot{Q}_w$ the heat exchanged through the wall.

Gas pressure reduction valve: this is an algebraic model that takes as inputs the income and outcome pressure, temperature and composition of the gas, and opening ratio of the valve φ , and returns the mass flow rate through the valve. The mass flow rate is calculated using the expansion factor Y, as

$$\dot{m} = N_x c_v Y \sqrt{\rho_{in}\Delta p}, \tag{7}$$

where N_x is a coefficient introduced to match the measurement units used.

Heat pump: this is an algebraic model in which the thermal power absorbed and that supplied by the heat pump are calculated based on the temperature of the cold and hot sources (T_c and T_h) and on the electrical power used P_{el}. The actual COP is calculated as follows

$$COP = \frac{COP_{nom}}{C_c(1-(1-C_c)}\frac{P_{el,nom}}{P_{el}}, \tag{8}$$

where C_c is a correction factor usually declared by the manufacturer, $COP_{nom} = \frac{COP_{max}}{\eta_{II}}$ and η_{II} is calculated with a lookup table with $\eta_{II} = f(T_c, T_h)$.

The inputs, outputs and states of the new components are reported in Table 1, while for the pumping station, heating network and thermal power unit blocks, the reader can refer to [12].

3. Application

This section describes the case study chosen and the main characteristics of the simulations. In addition, it presents how the control strategies have been implemented in the MiL application.

3.1. Case study description

The case study considered consists of a PtG plant for the production of synthetic methane, using the renewable electricity generated by a wind power plant. A simplified representation of the energy system is displayed in Figure 2.

The energy system is connected to the electrical grid and to the natural gas network, and it can exchange electricity and gas with them by buying and selling energy. The end-user has both electrical and thermal needs: the first are fulfilled by using the renewable electricity or by buying electricity from the power grid, while the latter are met with a gas-fueled boiler, and by recovering the waste heat from the PtG plant. Indeed, as mentioned above, two hot water circuits are employed: the HRC that works at low temperatures (40÷55) ℃, in which three heat exchangers recover the waste heat from the PEM electrolyzer (available at a temperature of 55 ℃), condenser (80 ℃) and methanation reactor (290 ℃), and the DHN which works at higher temperatures (60÷80) ℃ and is used for end-user heat supply (see Figure 1). An industrial heat pump (HP) connects the two circuits and upgrades the heat at 55 ℃ to the 80 ℃ needed for the DHN. The characteristics of the plants are shown in Table 2.

In Figure 2, all the energy flows involved are shown: the electricity produced by the wind farm can be used both for the fulfillment of the electrical needs, or by the PEM electrolyzer (PEM) that produces hydrogen,

Table 1: System components summary (Al = Algebraic, Dy = Dynamic).

Component	Model	Inputs	Outputs	States
Wind farm	Al	$\mathbf{u}_{wind}$	P_{el}	-
Electrolyzer	Al	P_{el} Op mode	$\dot{m}_{out}, T_{out}, x_{out}, p_{out}$ $\dot{m}_{H_2O}$, P_{th}, P_{loss}	-
Methanation reactor	Al	$\dot{m}_{in}, T_{in}, x_{in}$ Op mode	$\dot{m}_{out}, T_{out}, x_{out}$ P_{th}, P_{loss}	-
Gas compressor	Al	N, $p_{in}, p_{out}, T_{in}, x_{in}$	$\dot{m}_{out}, T_{out}, x_{out}, P_{el}$	-
Gas storage	Dy	$\dot{m}_{in}, T_{in}, x_{in}$	$p_{stor}, T_{stor}, x_{stor}$	$p_{stor}, T_{stor}, x_{stor}$
Gas pipeline	Dy	$p_{in}, T_{in}, x_{in}, p_{out}$	$\dot{m}_{out}, T_{out}, x_{out}$	T_{pipe}
Valve	Al	$p_{in}, T_{in}, x_{in}, p_{out}, \varphi$	$\dot{m}_{out}, T_{out}, x_{out}$	-
Heat pump	Al	T_h, T_c, P_{el}	$P_{th_{out}}, P_{th_{in}}$	-

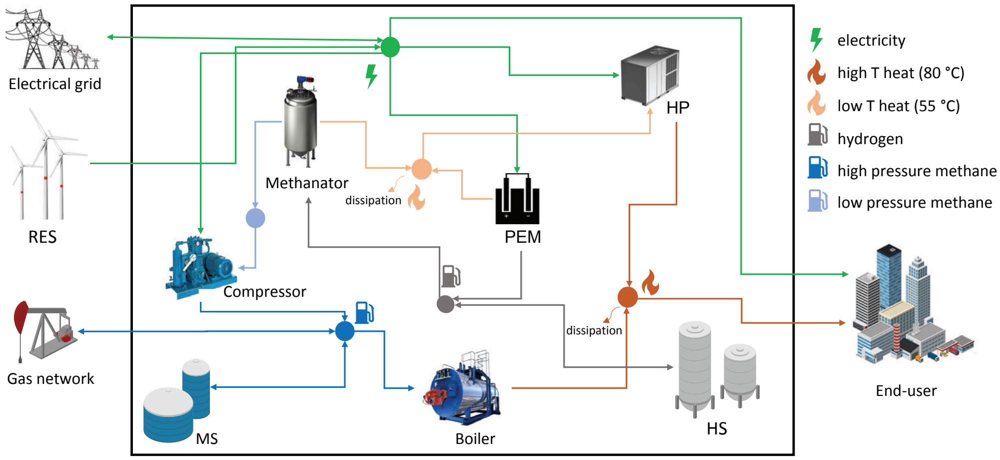

Figure 2: A schematic representation of the Multi-Energy System considered.

Table 2: Characteristics of the plants involved.

Technology	Parameter	Value	Technology	Parameter	Value
Wind farm	Number of turbines (-)	4	Boiler	Nominal inlet power (kW)	4000
	Nominal power (kW)	8000		Nominal efficiency (%)	92.4
Electrolyzer	Nominal inlet power (kW)	3750	Methanator	Nominal inlet power (kW)	2479
	Nominal operating temperature (℃)	55		Nominal operating temperature (℃)	290
	Nominal operating pressure (bar)	35		Nominal operating pressure (bar)	2.5
H_2 storage	Volume (m^3)	100	CH_4 storage	Volume (m^3)	100
	Maximum pressure (bar)	35		Maximum pressure (bar)	7.5
	Minimum pressure (bar)	2.5		Minimum pressure (bar)	3.5
Heat pump	Nominal inlet power (kW)	380			

and it is also consumed by the methane compressor and by the HP. The produced hydrogen can be stored in the hydrogen storage (HS) or used by the methanation reactor, which produces methane at low pressure (2.5 bar), which needs to be compressed before being used or stored in the methane storage (MS). After the compression, the methane can both be stored, sold, or used to feed the boiler, which produces the heat for end-user supply. In this work, the MPC controller is applied to a so-called system digital twin, which is a dynamic model, built by means of properly connecting the models of the single components involved which are developed in Simulink® and presented in Paragraph 2.3.. This allows the new control strategy to be tested, without affecting the operation of a real system. The controller is implemented as a supervisory controller, and gives the values of the manipulated variables calculated by the optimization algorithm as input set-points to low-level controllers (e.g. PID controllers) already implemented in the system.

3.2. Simulation setup

The main objective of this study is to compare the actual savings potential and the different management of the proposed MILP-based MPC with the use of a conventional rule-based control strategy. The following paragraphs present the two control strategies and describe how they are implemented.

3.2.1. MPC control

The schematic diagram of the MiL application of the MPC is shown in Figure 3: the MPC was set with a prediction horizon of two days and a time-step of one hour. At each time-step, the controller (i) gets the actual value of the system initialization variables, (ii) updates the forecast of the disturbances and the initial conditions and (iii) calls the optimization algorithm, which is run and returns the values of the optimal control variables as a result. The initialization and control variables, as well as the disturbances are described in Figure 3.

The objective function implemented is the maximization of the total operating margin of the system, which includes the costs of the electricity and natural gas bought and sold from/to the networks. The MILP algorithm described in Paragraph 2.2. was developed and adapted to the case study presented. The features of the linearization conducted to formulate the MILP algorithm are shown in Table 3, where it is specified whether or not the piecewise linearization has been conducted, its dimension, as well as the number of intervals employed. In addition, it is indicated if the UT, DT and operating ramps are modeled, as well as which operating modes are used.

The disturbances given to the MPC are the forecasts of end-user needs and the electrical power generated by the wind farm, and they are displayed in Figure 4 for the second simulated day. It is worth pointing out

https://doi.org/10.52202/069564-0221

that these forecasts are different from the disturbances applied to the Simulink® model, which represent the actual disturbances and are obtained by applying random deviations to the ideal disturbances given to the controller. In this way it is possible to evaluate how the predictive controller reacts to disturbances other than those expected, which usually happens in real applications.

3.2.2. Rule-based control

Depending on the definition of the conventional control strategy, the improvement due to management with the MPC control can vary, therefore a suitable and efficient rule-based control was developed. With this control strategy, the same set-points given by the MPC are calculated based on the logic displayed in Table 4.

It needs to be mentioned that the boiler set-point is not calculated with this control logic, and its input power is regulated through a PI controller, which keeps the supply temperature of the DHN equal to 80 °C. In addition, the actual amount of methane exchanged with the network is the set-point given for the methane sold minus the methane needed for the boiler.

3.3. Key Performance Indicators

To evaluate the results obtained, some Key Performance Indicators (KPIs) regarding the cumulative results of the second simulated day were analyzed. The KPIs identified are:

- Operating margin (EUR): the net revenue of the electricity and methane exchanged with the networks. Thus, it is the difference between the cost of the energy sold and the cost of the energy bought during the simulated period.
- CO_2 emissions ($kg_{CO_2,eq}$): the amount of carbon dioxide which is emitted due to the operation of the energy system. In particular, it considers the emissions related to the methane and electricity bought from the networks. Indeed, it was assumed that the electricity produced by the wind farm is associated with zero emissions, as well as the synthetic methane produced with the PtG plant. For the electrical grid, a coefficient of 224 gCO_2/kWh was considered [14], while for the gas 200.8 gCO_2/kWh [15].
- RES usage (%): the percentage of renewable electricity which is used by the system, and therefore not sold to the electrical grid.
- Gas production (kWh): the amount of methane produced by the Power-to-Gas system.
- Heat recovered share (%): the percentage of user thermal needs covered with the heat recovered from the PtG plant.

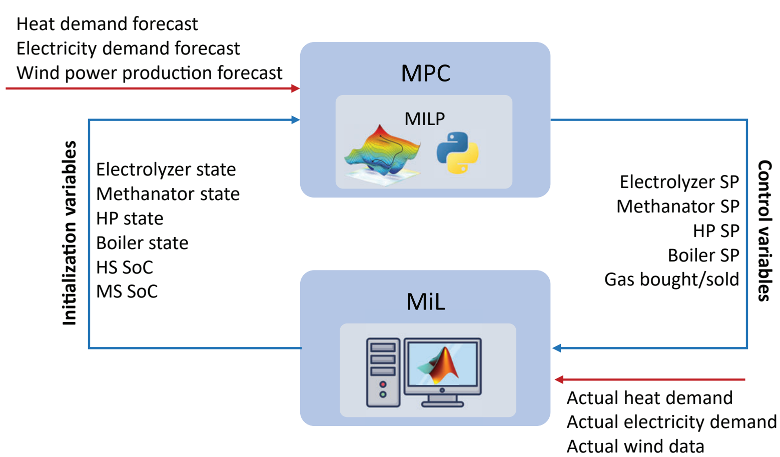

Figure 3: Model-in-the-Loop control with MPC (SP = set-point, SoC = State of Charge).

Table 3: Features of the model linearization for MILP formulation.

Component	Method	Intervals	Parameters	UT/DT	Ramps	Op. modes
Electrolyzer	piecewise 1D	1×3	$P_{out_{H_2}}, P_{out_{th}} = f(P_{in_{el}})$	no	no	ON/OFF/standby
Methanator	piecewise 1D	1×2	$P_{out_M}, P_{out_{th}} = f(P_{in_{H_2}})$	yes	yes	ON/OFF/standby
Gas compressor	piecewise 2D	2×2	$P_{in_{el}} = f(P_{in_{ng}}, E_{stor_{ng}})$	no	no	ON/OFF
Boiler	linear	1×1	$\eta_B = 92.2\,\%$	no	no	ON/OFF
Heat pump	linear	1×1	$COP = 5.42$	no	no	ON/OFF
H_2 storage	linear	1×1	$\eta_{ch} = \eta_d = 95\,\%$	-	-	-
Methane storage	linear	1×1	$\eta_{ch} = 95\,\%, \eta_d = 0.85\,\%$	-	-	-

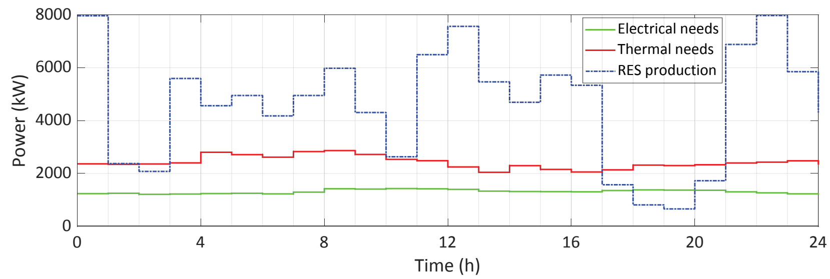

Figure 4: Forecasts of the disturbances given to the MPC controller for the second day.

Table 4: Rule-based control strategy definition.

Variable	Condition	Set-point value
Electrolyzer input power	$SoC_{HS} \leq 80\,\%$	$\min\{P_{nom}, (P_{wind} - P_{el_{user}})\}$
	otherwise	0
Methanator input power	$SoC_{HS} > 60\,\%$ & $SoC_{MS} \leq 95\,\%$	P_{nom}
	$SoC_{HS} > 60\,\%$ & $SoC_{MS} > 95\,\%$	0.5 P_{nom}
	otherwise	0
Heat pump input power	methanator ON & $P_{th_{user}} > 0$	P_{nom}
	otherwise	0
Methane sold	$SoC_{MS} > 70\,\%$	1200 kW
	$30\,\% \leq SoC_{MS} \leq 70\,\%$	600 kW
	$SoC_{MS} < 30\,\%$	0 kW

4. Results and discussion

As previously explained, the aim of the simulations is to test the benefits of a novel controller based on MPC applied to a PtG plant coupled with a DHN. In order to do so, the novel control strategy was compared to a conventional rule-based one (see Paragraph 3.2.). The simulations were carried out over two days: nevertheless, the rule-based control strategy is used in both simulations on the first day, in order to have the same initial conditions for the second day, in which the two control strategies are compared. Therefore, the results are collected during the second day and only these results will be discussed.

Figure 5 shows how the electricity is managed with the two control strategies during the second day: it displays the energy balance among production, usage and exchange with the grid. It is possible to note that with the MPC strategy, less electricity is exchanged with the grid, and the renewable electricity is mainly used to work the electrolyzer and the HP for heat recovery. Indeed, this can be also seen in Figure 6: here, the total amount of energy exchanged with the networks during the entire day is displayed. With the rule-based control, a larger amount of electricity is sold to the grid, and at the same time a larger amount of methane needs to be bought from the gas network. Indeed, when the electrolyzer and methanation reactor are not operating, it is necessary to buy the gas needed to work the boiler, in order to fulfill the thermal needs of the user. This result shows that

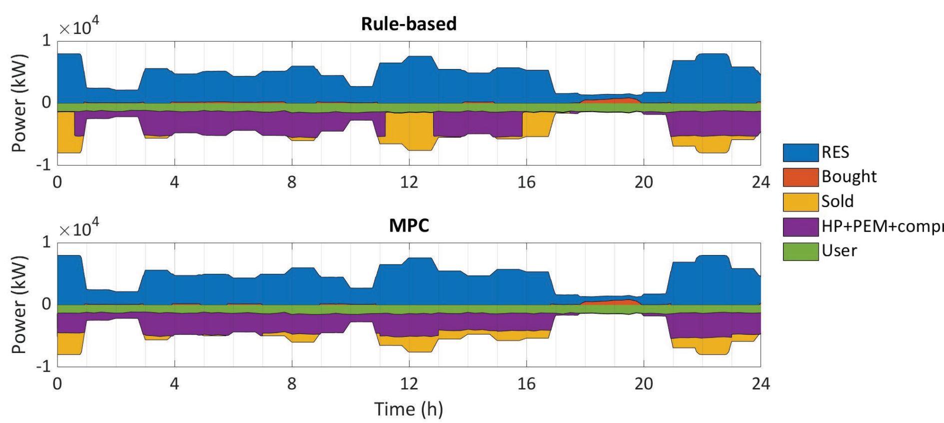

Figure 5: Energy balance at the electricity node (RES = wind power produced, Bought/Sold = exchanges with the power grid, HP = heat pump, PEM = PEM electrolyzer, compr = compressor, User = user needs).

 https://doi.org/10.52202/069564-0221

it is better to exploit the self-produced energy as much as possible and to reduce the energy exchanges with the networks to a minimum to obtain a cheaper operation for the system. In addition, with such management, grid unbalances are prevented, as well as renewable energy curtailments.

In Figure 7, both the set-point and the actual input power to the methanation reactor are shown. The set-point is the actual set-point exiting the low-level proportional controller, and thus takes into consideration a correction based on the behavior of the hydrogen storage that corrects it in order not to exceed the storage limits. It can be seen that with the two control strategies the management is different. In fact, with the rule-based control, the set-point is kept constant most of the time at part load, while with the MPC a more precise set-point can be defined, which allows makes it possible to optimally manage the system and minimize the objective function.

Figure 8 shows the actual input power of the electrolyzer with the two approaches, and the State of Charge of the hydrogen storage. Indeed, these two dimensions are strongly related to each other. It can be noted that with the rule-based control strategy there are some periods in which the electrolyzer must be switched off since the hydrogen storage is too full. This does not happen with the MPC, which can optimally manage the electrolyzer and switch it off only when there is not enough RES production (see Figure 4).

In Table 5 the values obtained for the KPIs identified in Paragraph 3.3. are displayed. As expected, the operating margin of the system is higher when the MPC is used, since its maximization is the objective implemented in the optimization, and in one day it is possible to increase the operating margin by 54 % (around 475 EUR). In addition, with the MPC better results are obtained also for the CO_2 emissions, which are more than halved compared with the ones obtained using the rule-based control. Furthermore, when looking at the RES usage,

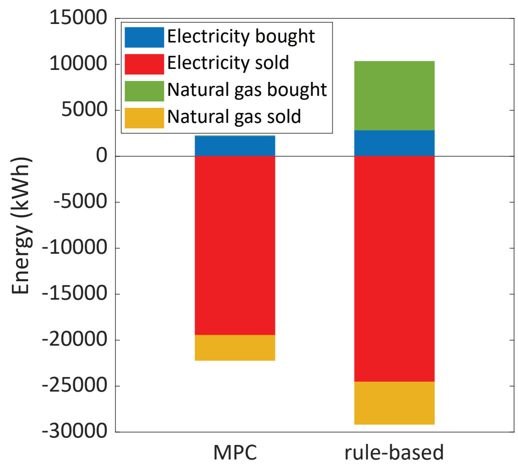

Figure 6: Bar plot with energy exchanged with the networks during the entire day.

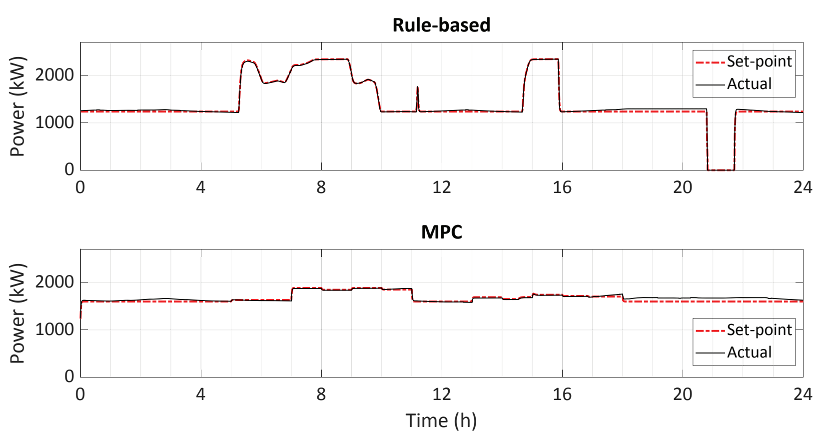

Figure 7: Input power set-point given to the methanation reactor with the two control strategies and actual input power.

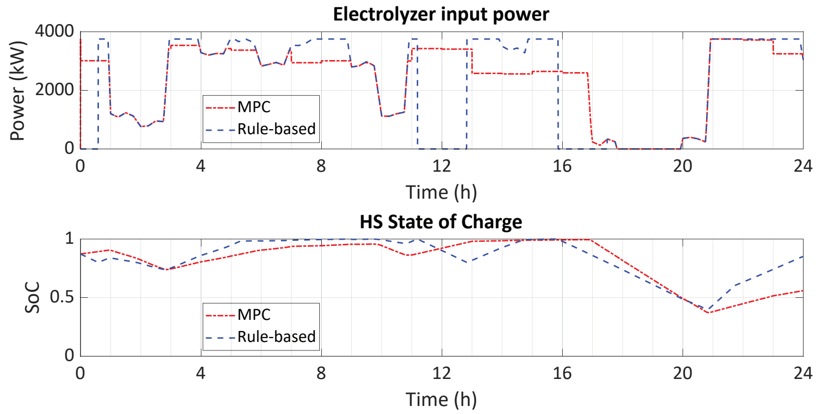

Figure 8: Actual input power of the electrolyzer and State of Charge of the hydrogen storage with the two control strategies.

Table 5: Values of the KPIs with the two control strategies.

Value	Rule-based control	MPC	Difference
Operating margin	874 EUR	1 349 EUR	**+ 475 EUR**
CO_2 emissions	2 139 $kg_{CO_2,eq}$	498 $kg_{CO_2,eq}$	**- 1 641** $kg_{CO_2,eq}$
RES usage	77.7 %	82.3 %	**+ 4.6 %**
Gas production	86 390 kWh	102 366 kWh	**+ 15 976 kWh**
Heat recovered share	42.0 %	44.8 %	**+ 2.8 %**

it is shown that with the MPC 4.6 % more renewable energy is exploited, and this leads also to a higher production of methane. Finally, the recovered heat is higher with the MPC: in particular with this strategy 44.8 % of the thermal demand is met by the recovered heat (2.8 % more than with the rule-based control).

It is worth noting that with the MPC better results are obtained for all the KPIs: this shows that maximizing the operating margin, the management of the system is more efficient under several aspects.

5. Conclusions

The energy transition is forcing the penetration of renewable energy sources and of new technologies into energy systems. Among them, Power-to-Gas solutions allow the production of synthetic fuels from renewable electricity, enable the storage of surplus electricity and permit sector integration. Due to these changes, energy systems are becoming increasingly complex and it is necessary to employ efficient and intelligent control strategies to manage them, in order to fully unlock the benefits of the novel solutions.

In this work, a controller based on Model Predictive Control was presented and it was applied to an integrated system with the production of methane from renewable electricity, with the objective of increasing the operating margin. Besides, a novel solution to recover the waste heat from Power-to-Gas exothermic components was proposed, which uses a heat pump to upgrade the heat available at low-temperature from the plant to the level of the supply temperature needed by a district heating network. The developed controller was tested in a Model-in-the-Loop configuration and compared to a traditional rule-based control strategy.

The results show that with the developed controller it is possible to have smarter energy management: indeed, the operation of the components and storage tanks is improved and the operating margin of the system is increased by 54 % in one day. In addition, with the novel controller 4.6 % more renewable electricity is exploited and the total emissions of carbon dioxide are strongly reduced, compared with the rule-based control.

Future studies will examine how the controller performs when adapted to different case studies and the use of different objective functions, which may include the minimization of energy consumption or carbon dioxide emissions. Furthermore, to fully understand the possible role of Power-to-Gas in the energy transition toward a sustainable energy framework, its potential as a long-term storage solution needs to be identified. To do that, the developed controller will be coupled with a supervisory controller, based on Model Predictive Control, which will provide it with further constraints regarding the correct long-term operation of the system. In this way, it would be possible to fully exploit the capabilities of Power-to-Gas as a seasonal storage solution.

https://doi.org/10.52202/069564-0221

Nomenclature

A_{cs}	Cross-section area of pipeline, m^2
C_c	Correction factor, $-$
c_p	Specific heat at constant pressure, $J/(kgK)$
c_v	Specific heat at constant volume, $J/(kgK)$
D_{in}	Inner diameter of pipeline, m
DT	Down-Time
DHN	District Heating Network
E	Energy, kWh
HHV	High Heating Value, kJ/kg
HRC	Heat Recovery Circuit
KPIs	Key Performance Indicators
L	Length of pipeline, m
λ	Friction factor, $-$
$\dot{m}$	Mass flow rate, kg/s
MES	Multi-Energy System
MiL	Model-in-the-Loop
MILP	Mixed-Integer Linear Programming
MPC	Model Predictive Control
N	Rotational speed, rpm
η	Efficiency, $-$
P	Power, kW
p	Pressure, Pa
PtG	Power-to-Gas
φ	Valve opening ratio,
$\dot{Q}_w$	Heat lost through wall, J/s
ρ	Density, kg/m^3
SoC	State of Charge
t	Time, h
T	Temperature, K
$\mathbf{u}$	Velocity, m/s
UT	Up-Time
V	Volume, m^3
$\dot{V}$	Volumetric flow rate, m^3/s
x	Mole fraction, $-$
y	Yield of reaction, $-$
Y	Valve expansion factor, $-$
Z	Total concentrated pressure drop through the pipeline, Pa

Subscripts and superscripts

c	cold
ch	charge
d	discharge
el	electrical

https://doi.org/10.52202/069564-0221

h hot

in input

nom nominal

out output

stor stored

th thermal

References

[1] Marzi, E., Morini, M., Gambarotta, A., *Analysis of the status of research and innovation actions on electrofuels under horizon 2020*. Energies 2022;15(2), 618.

[2] Böhm, H., Moser, S., Puschnigg, S., Zauner, A., *Power-to-hydrogen & district heating: Technology-based and infrastructure-oriented analysis of (future) sector coupling potentials*. International Journal of Hydrogen Energy 2021;46(63), 31938-31951.

[3] Fischer, D., Kaufmann, F., Hollinger, R., Voglstätter, C., *Real live demonstration of MPC for a power-to-gas plant*. Applied Energy 2018;228, 833-842.

[4] Turk, A., Wu, Q., Zhang, M., *Model predictive control based real-time scheduling for balancing multiple uncertainties in integrated energy system with power-to-x*. International Journal of Electrical Power & Energy Systems 2021;130, 107015.

[5] Abdelghany, M. B., Shehzad, M. F., Mariani, V., Liuzza, D., Glielmo, L., *Two-stage model predictive control for a hydrogen-based storage system paired to a wind farm towards green hydrogen production for fuel cell electric vehicles*. International Journal of Hydrogen Energy 2022;47(75), 32202-32222.

[6] Huang, C., Zong, Y., You, S., Træholt, C., *Economic model predictive control for multi-energy system considering hydrogen-thermal-electric dynamics and waste heat recovery of MW-level alkaline electrolyzer.* Energy Conversion and Management 2022;265, 115697.

[7] Blaud, P. C., Haurant, P., Claveau, F., Lacarrière, B., Chevrel, P., Mouraud, A., *Modelling and control of multi-energy systems through multi-prosumer node and economic model predictive control*. International Journal of Electrical Power and Energy Systems 2020;118, 105778.

[8] Urbanucci, L., *Limits and potentials of Mixed Integer Linear Programming methods for optimization of polygeneration energy systems.* ATI 2018: Proceedings of the 73rd Conference of the Italian Thermal Machines Engineering Association; 2018 Sept 12-14; Pisa, Italy. Energy Procedia, 148, 1199-1205.

[9] Maier, L., Schönegge, M., Henn, S., Hering, D., Müller, D., *Assessing mixed-integer-based heat pump modeling approaches for model predictive control applications in buildings.* Applied Energy 2022;326, 119894.

[10] Bischi, A., Taccari, L., Martelli, E., Amaldi, E., Manzolini, G., Silva, P., Campanari, S., Macchi, E. , *A detailed MILP optimization model for combined cooling, heat and power system operation planning*. Energy 2014;74, 12-26.

[11] D'Ambrosio, C., Lodi, A., Martello, S., *Piecewise linear approximation of functions of two variables in MILP models*. Operations Research Letters 2010;38(1), 39-46.

[12] De Lorenzi, A., Gambarotta, A., Morini, M., Rossi, M., Saletti, C., *Setup and testing of smart controllers for small-scale district heating networks: An integrated framework*. Energy 2020;205, 118054.

[13] Yang, K., Kwak, G., Cho, K., Huh, J., *Wind farm layout optimization for wake effect uniformity*. Energy 2019;183, 983-995.

[14] Statista 2023. *Carbon intensity of the power sector in Italy from 2000 to 2021* Available at: `https://www.statista.com/statistics/1290244/carbon-intensity-power-sector-italy/` [accessed 14.3.2023].

[15] volker-quaschning.de. *Specific carbon dioxide emissions of various fuels* Available at: `https://www.volker-quaschning.de/datserv/CO2-spez/index_e.php` [accessed 14.3.2023]

https://doi.org/10.52202/069564-0221